Determining the Best Fit Halo Density Profile of the Milky Way-M31 Remnant

Alessandro Bressani, May 8th, 2025[1]

[1]*Steward Observatory, Department of Astronomy, University of Arizona, 933 N. Cherry Ave, Tucson, AZ 85721, USA*

ABSTRACT

Dark matter halos gravitationally attract baryons and mark the location of galaxy formation. Studying these halos is crucial for testing and improving ΛCDM cosmology, the leading paradigm of cosmic structure and evolution. GADGET-3 is a collisionless, hydrodynamical N-body simulation that represents the initial dark matter halo of the Milky Way and M31 in a Hernquist profile. The simulation can be used to analyze the Milky Way-M31 merger remnant density profile and determine if the Hernquist profile or the NFW profile is a better fit. The Hernquist profile was found to provide a better fit for the merger remnant compared to the NFW profile, with an average residual of -3.97×10^{-5} (verses -1.3×10^{-4} for the NFW profile). Using the parameters of the Hernquist profile, this project sets the groundwork for further analysis on the structure and kinematics of dark matter halos. This, by extension, allows us to further test and improve ΛCDM.

Keywords: Dark Matter Halo, Cold Dark Matter Theory, Critical Density, Hernquist Profile, NFW Profile, N-body Simulations, Major Merger, Elliptical Galaxy

1. INTRODUCTION

Dark matter (DM) halos are virialized collections of dark matter that are not affected by the expansion of the universe. They gravitationally attract baryons and therefore mark the site of galaxy formation (private communication, G. Besla, May 6, 2024). Dark matter particles are thought to be collisionless, allowing them to conserve their orbital energy and support themselves through dispersion (A. R. Wetzel & D. Nagai 2015). Studying the density profiles of DM halos is one method to constrain the nature of DM halos and particles (J. Prada et al. 2019). Understanding this is crucial for testing and improving **lambda cold dark matter (ΛCDM) theory**, the leading paradigm for cosmic structure and evolution (see following paragraph).

Galaxies are collections of stars, stellar remnants, gas, dust, and dark matter whose kinematics cannot be explained by visible matter (L. S. Sparke & J. S. Gallagher 2000). They appear to have missing, or 'dark' matter that allows stars to remain gravitationally bound. ΛCDM theory describes dark matter as cold and slow, allowing for hierarchical galaxy growth (C. S. Frenk & S. D. M. White 2012). The Λ refers to the cosmological parameters outlined by Planck Collaboration et al. (2016) where $h = H_0/(100\, kms^{-1}Mpc^{-1}) = 0.6727, \Omega_m = 0.3156, \Omega_\Lambda = 0.6844, \Omega_b = 0.04927$. These parameters are used to define ρ_{crit}, or the **critical density** for the expansion of the universe to eventually halt ($\rho_{crit} = 3H_0^2/8\pi G = 1.277 \times 10^{-8}\ (10^{10} M_\odot\ kpc^{-3})$). ΛCDM has been largely successful in describing the history, structure, and evolution cosmos, but can be improved by further investigating the nature of DM halos. Given their significance in the assembly of DM halos, *galaxy mergers* offer a unique perspective to peer into the nature of *galaxy evolution*. Galaxy evolution pertains to the processes that guide the development of galaxies such as star formation, gas accretion, or galaxy mergers.

Within ΛCDM theory, the **Hernquist profile** from L. Hernquist (1990) (See Section 3.3.1) and **Navarro-Frenk-White (NFW) density profile** from J. F. Navarro et al. (1997) (See Section 3.3.2) are commonly used to describe DM halos. These profiles were formulated with the aid of **N-body simulations** (See Section 3.1). N-body simulations simplify complex systems with multiple components, such as DM halos, that would be impossible to study with absolute precision. C. S. Frenk & S. D. M. White (2012) used a number of N-body simulations, such as the Aquarius simulation seen in **Figure 1**, to determine that the mass of halos is concentrated toward the center, aspherical, and contains substructures especially in the outermost regions. It was also found from M. Davis et al. (1985) that CDM halos are often triaxial and rotate slowly.

Dark matter halos contract as a result of galaxy formation. G. R. Blumenthal et al. (1986) established

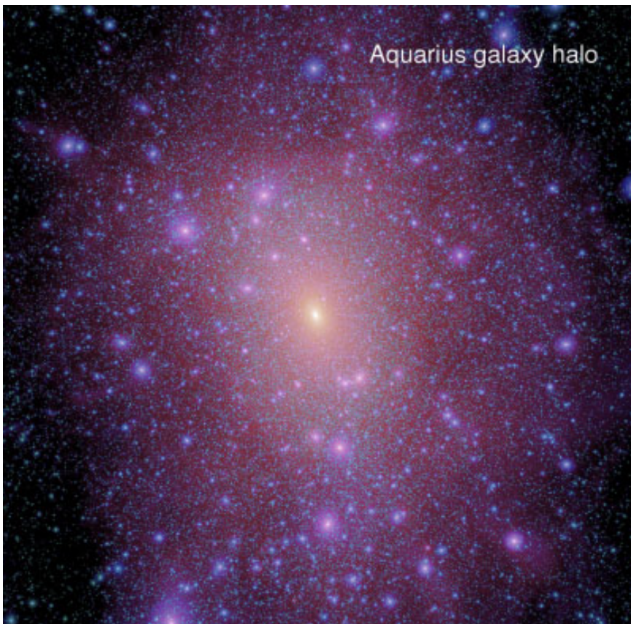

Figure 1. Simulated dark matter halo from C. S. Frenk & S. D. M. White (2012). Aquarius galaxy has similar mass to the Milky Way. Note primary structure of high density at the core and decreasing density as a function of distance from the core.

a mostly-accurate formula linking mass profiles before and after galaxy assembly assuming adiabatic invariants, however this 'adiabatic contraction' hypothesis has been found to overestimate simulated results (C. S. Frenk & S. D. M. White 2012). A. A. Dutton et al. (2007) proposed possible solutions for this problem that revised the hypothesis to reduce or even reverse this contraction. Additionally, ΛCDM faces challenges such as the cusp-core problem (first observed by R. A. Flores & J. R. Primack 1994). Simulated results suggest that DM halos have a sharp "cusp" at small radii. However, observations of velocity curves have suggested that certain galaxies, especially dwarf galaxies, have much flatter cores (See review by J. S. Bullock & M. Boylan-Kolchin 2017). To investigate these problems, a wider understanding of DM halos is needed, such as their kinematics, how they respond to galaxy growth, and orbital structures. Answering these questions involves understanding the nature of the halo density profiles and defining a model as a basis to further examine DM halos.

2. THIS PROJECT

Simulating the Milky Way and M31 **major merger** event opens a unique opportunity to study galaxy formation. Major merger refers to galaxy collisions where the mass ratio between the galaxies is greater than 1:10 (C. S. Frenk & S. D. M. White 2012). Because of the vast amount of information we can obtain from the Milky Way and M31, it is the most accurate simulation achievable for merger events, allowing for an incredibly in-depth analysis of the characteristics of galaxies, galaxy formation, and the evolution of the universe. In this project, I will compare the Hernquist and NFW halo density profiles with simulated results using the GADGET-3 N-body simulation of the Milky Way and M31 merger.

Determining the best-fit profile will provide additional insight into the processes that could mitigate or reverse adiabatic contraction. Specifically, models can be used to describe the halo virial velocities that can affect the contraction of a halo during galaxy evolution (A. A. Dutton et al. 2007). Furthermore, the density profile can be used to determine if the merger remnant suffers from the cusp-core problem.

Studying the adiabatic compression and cusp-core problems allow for further constraints to be placed on DM halos and the DM particle. This allows ΛCDM to be tested and improved. In turn, we will improve our understanding of galaxy assembly/evolution and the nature of the cosmos.

3. METHODOLOGY

3.1. *N-body Simulation (P1)*

The GADGET-3 N-body simulation is a collisionless, hydrodynamical N-body simulation that represents the initial dark matter halo of each galaxy as a Hernquist profile (R. P. van der Marel et al. 2012). The use of a Hernquist profile allows for a finite DM halo mass (V. Springel 2005), and the omission of collisions allows for a defined, unchanging energy in the system. This is ideal for simplifying N-body simulations, which model complex, dynamic systems with many parts.

Setup of the Milky Way and M31 merger can be seen in Table 1 (from R. P. van der Marel et al. 2012). Values for the masses, radii, and position angles are derived from observational results. Simulation particles are separated into disk, bulge, and halo particles that interact gravitationally. For simplification, the Milky Way is initially at rest at the origin of the simulation.

3.2. *Approach (P2)*

For proper analysis, I want to take the *equilibrium* density profiles of the remnant, so I will analyze the final high resolution snap number (801) of the *halo* component for the merged Milky Way and M31 galaxies. Because the data from both galaxies is a text file, I can manually append the 801 snap numbers for the Milky Way and M31 together.

Quantity	Milky Way	M31	Source
Inclination (deg)	...	77.5	(a),(b)
R_{disk} (kpc)	3.0	5.0	(c)
R_{bulge} (kpc)	0.6	1.0	...
M_{bulge} (10^{10} $M_\odot$)	1.0	1.9	(c)
N_{dark}	500,000	500,000	...
N_{disk}	750,000	1,200,000	...
N_{bulge}	100,000	190,000	...

Table 1. Observationally derived setup details of the GADGET-3 N-body simulation of the Milky Way and M31 merger from R. P. van der Marel et al. (2012). R refers to radius; M refers to mass; N refers to number of particles. Simulation particles are separated into disk, bulge, and halo particles that interact gravitationally. Sources are (a) L. Chemin et al. (2009); (b) E. Corbelli et al. (2010); (c) A. Klypin et al. (2002).

Using the merged data, I define the center of mass of the halo and consider spherical shells from 3 kpc to R_{200} with step size $dr = 0.01$ from the center of mass. Starting at 3 kpc avoids the cusp of the halo and the low resolution that occurs near the core. R_{200} is defined as the radius in which the density is 200 times the critical density of the universe, ρ_{crit}. Beyond R_{200}, the halo is considered too diffuse and no longer physical. Initial calculations determined $R_{200} = 278.737$ kpc. Using these spheres, I will sum the masses of the halo particles within and find the density as a function of radius from the center of mass.

3.3. *Density Profiles (P3)*

3.3.1. *Hernquist Profile*

The Hernquist density profile was derived from the spherical galaxy density profile from W. Jaffe (1983) and is proportional to r^{-4}. The Hernquist density profile given by **Equation 1**, where a is a scale length and M_{halo} is the total mass of the halo (L. Hernquist 1990).

$$\rho(r) = \frac{M_{halo}}{2\pi} \frac{a}{r(r+a)^3} \tag{1}$$

To fit the Hernquist profile, I will use the total mass of halo the particles in the simulation as M_{halo} and let a be a free parameter. We can expect a to be between 10 and 80 kpc.

3.3.2. *NFW Profile*

The Milky Way and M31 merger remnant is theorized to be a large **elliptical galaxy** (R. P. van der Marel et al. 2012). Elliptical galaxies are are supported by dispersion and exhibit low star formation rates (S. M. Faber & R. E. Jackson 1976; W. J. Pearson et al. 2019).

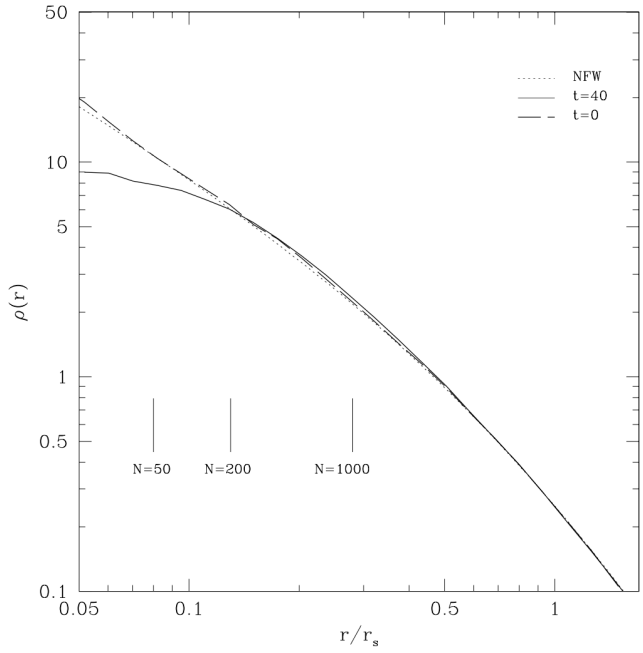

Figure 2. Example of NFW density profile. Here, r_s is scale radius. Vertical lines represent where 50, 200, and 1000 halo particles are encompassed. t refers to the crossing time of a particle at r_{max} and V_{max} (see Eq. 6 in A. Klypin et al. 2013). NFW density profiles assume a r^{-3} radial dependence. The goal of this project is to determine which profile between Hernquist and NFW is a better fit.

The density profiles of large elliptical halos can be fit to an NFW profile (as described by C. S. Frenk & S. D. M. White 2012)) outlined in **Equation 2**. NFW profiles are proportional to r^{-3}. Here, ρ_s is the characteristic density and r_s is the characteristic radius. An example of a NFW density profile can be seen in **Figure 2**.

$$\rho(r) = \rho_{dm} \left(\frac{r}{r_{dm}}\right)^{-1} \left(1 + \frac{r}{r_{dm}}\right)^{-2} \tag{2}$$

To model the NFW profile, I consider the halo concentration, $c = R_{200}/r_s$. Typical halo concentrations are between 15 and 20 (G. Besla, private communication, May 6, 2025). For a plausible halo concentration and considering $R_{200} = 278.737$ kpc, I need to select a characteristic density that returns a best fit r_s between $\sim$18 and $\sim$28 kpc. I will select this characteristic density from the Hernquist best-fit density array. This allows for ample freedom for the NFW best fit while upholding plausible parameter values.

3.4. *Curve-fitting models (P4)*

SciPy curve-fit allows the user to fit a function to data via a non-linear least-squares fit and return the best-

fit values of the function's parameters. After fitting the Hernquist and NFW profiles to the remnant's DM halo density profile, I will examine the average residual between the models and the simulation to determine which profile provides the best fit for the halo remnant. I will also graph the profiles and residuals to visualize the best fit and the simulation results.

The first resulting figure will be an image of the halo at snap 801 using a simple 2D histogram. R_{200} will be outlined to get a sense of scale of the halo and contextualize the density profiles. The second figure will be the simulated and best-fit Hernquist and NFW density profiles. The best-fit parameters (a and r_s) for each profile will be included. I will also provide a plot of the residuals of each model with respect to radius. This will be provided as a visual aid when determining the best-fit profile.

3.5. *Hypothesis (P5)*

Due to the Hernquist profile's vital role in initializing the simulation, I hypothesize that it will be the best fit after the merger has occurred and virial equilibrium is reached.

4. RESULTS

The dark matter halo of the Milky Way and M31 merger remnant can be seen in **Figure 3**. Here, R_{200} is marked by the white circle. Although the halo is no longer physical beyond this radius, particles extend out to $\sim 10,000$ kpc. It can be seen that the halo increases concentration towards the center. How this density changes as a function of distance from the core is the aim of this project.

Figure 4 presents the Milky Way M31 remnant density profile and the curve fit results. For the Hernquist profile, $M_{halo} \approx 412 \times 10^{10} M_\odot$ and $a \approx 18.63$ kpc. The average residual for the Hernquist profile was -3.97×10^{-5}. For the NFW profile, $\rho_s \approx 5.230259 \times 10^{-3}$ $(10^{10} M_\odot / kpc^3)$ and $r_s \approx 24.14\, kpc$. This allowed a halo concentration of $c = 11.54$ The average residual for the NFW profile was -1.3×10^{-4}. Because the average residual was smaller for the Hernquist profile, I conclude that the Hernquist profile was the better fit for the remnant density profile.

5. DISCUSSION

5.1. *Hernquist Profile*

For the Hernquist profile from **Equation 1**, I found $M_{halo} \approx 412 \times 10^{10} M_\odot$ from the simulation. SciPy curve fit determined $a \approx 18.63\, kpc$ to produce the best fit for the model function. This returned an average residual of -3.97×10^{-5}. The low residual suggests that this result agrees with my hypothesis.

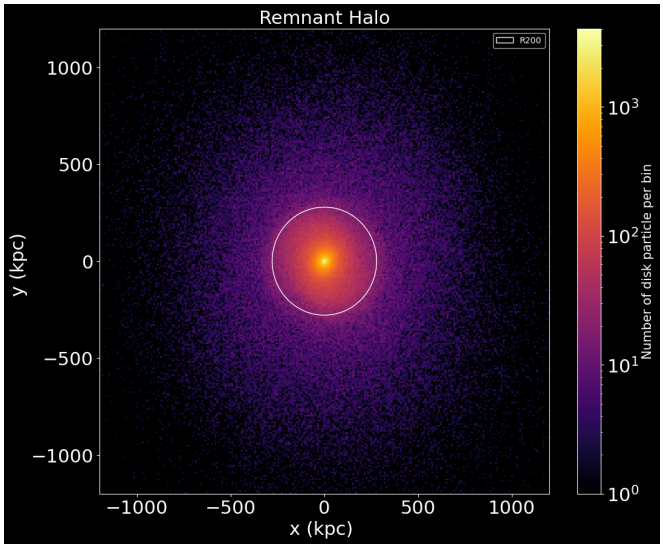

Figure 3. Dark matter halo of the Milky Way and M31 merger remnant. Axes refer to distance in kpc centered on the center of mass of the halo. The white circle represents $R_{200} = 278.737$ kpc, where the halo density within is 200 times the critical density of the universe. Beyond this point the halo can be considered no longer physical, though dark matter particles can still be found extended out to $\sim 10,000$ kpc. All profile fitting will apply from 3 kpc to R_{200}.

R. P. van der Marel et al. (2012) set up their simulation in a Hernquist profile with the advantage of having a finite total mass. Considering the finite, albeit larger total mass in the merger remnant, it is consistent for the remnant to fit to a Hernquist profile well. J. S. Bullock & K. V. Johnston (2005) also found Hernquist profiles to fit well to their N-body simulations of Milky Way-like galaxies. L. Hernquist (1990) uses scale length, a, to describe the mass profile, kinematics, and dynamics of the halo. These results can be used to study the hierarchical growth of galaxies.

The scale length, a, for the Milky Way and M31 were set to 62.5 kpc (R. P. van der Marel et al. 2012). We can therefore expect a remnant scale length of similar magnitude. However, $a \approx 18.63\, kpc$ is lower than expected and may raise questions about the efficacy of the curve fitting.

5.2. *NFW Profile*

For the NFW profile from **Equation 2**, I used the characteristic density of the halo, ρ_s, as a fixed parameter and the characteristic radius, r_s, as free parameter for the best fit. To return a plausible halo concentration (as outlined in Section 3.3.2), a characteristic density of $\rho_s = 5.23 \times 10^{-3}$ $(10^{10} M_\odot / kpc^3)$ was chosen. SciPy curve fit determined $r_s \approx 24.14\, kpc$ to produce the best fit for the model function. This returned an average

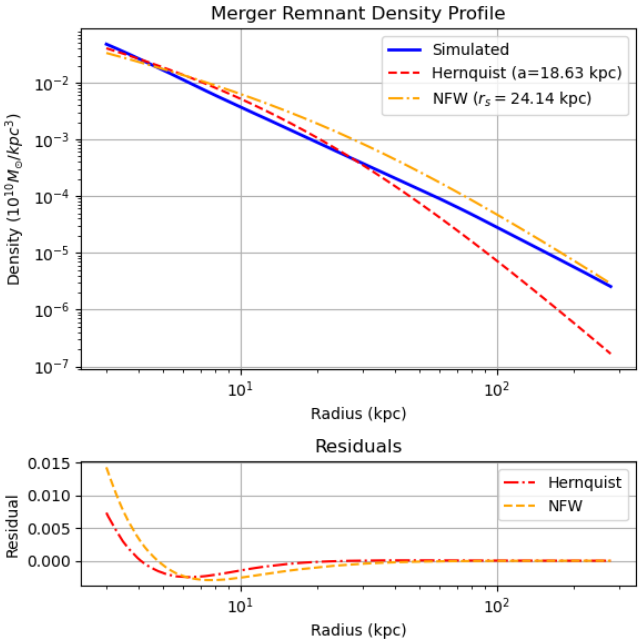

Figure 4. Top: Density profile of merger remnant and best fit results. X-axis is radial distance from halo center of mass, and y-axis is spherical density in units of $10^{10} M_\odot/kpc^3$. Blue solid line is simulated density profile, red dashed line is Hernquist fit, and orange dot-dashed line is NFW fit. Best-fit values for parameters are listed in the legend; a refers to a scale radius for the Hernquist profile and r_s refers to a characteristic radius for the NFW profile. Bottom: Residual plot between best-fit model and simulated density profile. X-axis is radial distance in kpc from halo center of mass; y-axis is the difference between simulated and modeled density profile. Red dashed line is Hernquist residual and orange dot-dashed line is NFW residual. The average residual for the Hernquist profile is -3.97×10^{-5} and -1.3×10^{-4} for the NFW profile, indicating that the Hernquist profile is the better fit.

residual of -1.3×10^{-4}. This residual is not lower than the Hernquist profile. Therefore, this result agrees with my hypothesis.

J. F. Navarro et al. (1997) found with N-body simulations that all DM halos follow the NFW model regardless of mass. This is the case in a universe with cold dark matter and hierarchical growth. This profile is proportional to the density of the universe at the time of halo assembly (J. F. Navarro et al. 1997), emphasizing the link between evolution of the halo and the profile. My results suggested that the NFW provided a good fit to the density profile, confirming its ubiquity.

The characteristic density (ρ_s) was selected so that the concentration (c) would be a plausible value. My methodology allows the constraining of one parameter, however this parameter was constrained in a way so that r_s could be constrained between $\sim$ 18.58 and $\sim$ 13.94 (allowing c to fall between 15 and 20). This suggests less freedom for both parameters in the hope of obtaining plausible parameter results. However, this was necessary as earlier curve fiting placed r_s and c at unrealistically high or low results.

6. CONCLUSIONS

Dark matter halos gravitationally attract baryons and mark the location of galaxy formation. Studying these halos is crucial for testing and improving ΛCDM cosmology, the leading paradigm of cosmic structure and evolution. GADGET-3 is a collisionless, hydrodynamical N-body simulation that represents the initial dark matter halo of the Milky Way and M31 in a Hernquist profile. The simulation can be used to analyze the Milky Way-M31 remnant density profile and determine if the Hernquist profile or the NFW profile is a better fit.

It was found that both the Hernquist and NFW profiles provided a strong fit for the remnant density profile with average residuals near zero. However, the Hernquist profile provided a better overall fit. This result agreed with my hypothesis. Using the best-fit parameters of the Hernquist profile, further studies on the structure and kinematics of the remnant DM halo can address the adiabatic compression and cusp-core problem, improving ΛCDM theory.

The initial aim of this project was to use the best-fit parameters to determine the expected velocity dispersion curve of the remnant. This would address if the merger remnant suffers from the cusp-core problem of ΛCDM and place constraints on the galaxy mass where this problem appears.

7. ACKNOWLEDGMENTS

Thank you to Dr. Gurtina Besla and Himansh Rathore for their patient and continuous guidance and expertise during this project. I am also grateful for the help given by Isabella Olin and the graduate student body at Steward Observatory.

This work used the following software packages: `astropy` (Astropy Collaboration et al. 2013, 2018, 2022), `matplotlib` (J. D. Hunter 2007), `numpy` (C. R. Harris et al. 2020), `python` (G. Van Rossum & F. L. Drake 2009), and `scipy` (P. Virtanen et al. 2020; R. Gommers et al. 2025). Software citation information aggregated using `The Software Citation Station` (T. Wagg & F. S. Broekgaarden 2024; T. Wagg et al. 2024).

We respectfully acknowledge the University of Arizona is on the land and territories of In- digenous peoples. Today, Arizona is home to 22 federally recognized tribes, with Tucson being home to the O'odham and the Yaqui. The University strives to build sustainable

relation- ships with sovereign Native Nations and Indigenous communities through education offerings, partnerships, and community service.

REFERENCES

Astropy Collaboration, Robitaille, T. P., Tollerud, E. J., et al. 2013, A&A, 558, A33, doi: 10.1051/0004-6361/201322068

Astropy Collaboration, Price-Whelan, A. M., Sipőcz, B. M., et al. 2018, AJ, 156, 123, doi: 10.3847/1538-3881/aabc4f

Astropy Collaboration, Price-Whelan, A. M., Lim, P. L., et al. 2022, ApJ, 935, 167, doi: 10.3847/1538-4357/ac7c74

Blumenthal, G. R., Faber, S. M., Flores, R., & Primack, J. R. 1986, ApJ, 301, 27, doi: 10.1086/163867

Bullock, J. S., & Boylan-Kolchin, M. 2017, ARA&A, 55, 343, doi: 10.1146/annurev-astro-091916-055313

Bullock, J. S., & Johnston, K. V. 2005, ApJ, 635, 931, doi: 10.1086/497422

Chemin, L., Carignan, C., & Foster, T. 2009, ApJ, 705, 1395, doi: 10.1088/0004-637X/705/2/1395

Corbelli, E., Lorenzoni, S., Walterbos, R., Braun, R., & Thilker, D. 2010, A&A, 511, A89, doi: 10.1051/0004-6361/200913297

Davis, M., Efstathiou, G., Frenk, C. S., & White, S. D. M. 1985, ApJ, 292, 371, doi: 10.1086/163168

Dutton, A. A., van den Bosch, F. C., Dekel, A., & Courteau, S. 2007, ApJ, 654, 27, doi: 10.1086/509314

Faber, S. M., & Jackson, R. E. 1976, ApJ, 204, 668, doi: 10.1086/154215

Flores, R. A., & Primack, J. R. 1994, ApJL, 427, L1, doi: 10.1086/187350

Frenk, C. S., & White, S. D. M. 2012, Annalen der Physik, 524, 507, doi: 10.1002/andp.201200212

Gommers, R., Virtanen, P., Haberland, M., et al. 2025,, v1.15.2 Zenodo, doi: 10.5281/zenodo.14880408

Harris, C. R., Millman, K. J., van der Walt, S. J., et al. 2020, Nature, 585, 357, doi: 10.1038/s41586-020-2649-2

Hernquist, L. 1990, ApJ, 356, 359, doi: 10.1086/168845

Hunter, J. D. 2007, Computing in Science & Engineering, 9, 90, doi: 10.1109/MCSE.2007.55

Jaffe, W. 1983, MNRAS, 202, 995, doi: 10.1093/mnras/202.4.995

Klypin, A., Prada, F., Yepes, G., Hess, S., & Gottlober, S. 2013, arXiv e-prints, arXiv:1310.3740, doi: 10.48550/arXiv.1310.3740

Klypin, A., Zhao, H., & Somerville, R. S. 2002, ApJ, 573, 597, doi: 10.1086/340656

Navarro, J. F., Frenk, C. S., & White, S. D. M. 1997, ApJ, 490, 493, doi: 10.1086/304888

Pearson, W. J., Wang, L., Alpaslan, M., et al. 2019, A&A, 631, A51, doi: 10.1051/0004-6361/201936337

Planck Collaboration, Ade, P. A. R., Aghanim, N., et al. 2016, A&A, 594, A13, doi: 10.1051/0004-6361/201525830

Prada, J., Forero-Romero, J. E., Grand, R. J. J., Pakmor, R., & Springel, V. 2019, MNRAS, 490, 4877, doi: 10.1093/mnras/stz2873

Sparke, L. S., & Gallagher, III, J. S. 2000, Galaxies in the universe : an introduction

Springel, V. 2005, MNRAS, 364, 1105, doi: 10.1111/j.1365-2966.2005.09655.x

van der Marel, R. P., Besla, G., Cox, T. J., Sohn, S. T., & Anderson, J. 2012, ApJ, 753, 9, doi: 10.1088/0004-637X/753/1/9

Van Rossum, G., & Drake, F. L. 2009, Python 3 Reference Manual (Scotts Valley, CA: CreateSpace)

Virtanen, P., Gommers, R., Oliphant, T. E., et al. 2020, Nature Methods, 17, 261, doi: 10.1038/s41592-019-0686-2

Wagg, T., Broekgaarden, F., & Gültekin, K. 2024,, v1.2 Zenodo, doi: 10.5281/zenodo.13225824

Wagg, T., & Broekgaarden, F. S. 2024, arXiv e-prints, arXiv:2406.04405. https://arxiv.org/abs/2406.04405

Wetzel, A. R., & Nagai, D. 2015, ApJ, 808, 40, doi: 10.1088/0004-637X/808/1/40